Original Article

GA3, a new gambogic acid derivative, exhibits potent antitumor activities *in vitro via* apoptosis-involved mechanisms

Hua XIE[1], Yu-xin QIN[1], Yun-long ZHOU[2], Lin-jiang TONG[1], Li-ping LIN[1], Mei-yu GENG[1], Wen-hu DUAN[2*], Jian DING[1*]

[1]Division of Antitumor Pharmacology and [2]Department of Medicinal Chemistry; State Key Laboratory of Drug Research, Shanghai Institute of Materia Medica, Chinese Academy of Sciences, Shanghai 201203, China

Aim: Gambogic acid (GA) is the major active ingredient of gamboge, which is secreted from a Chinese traditional medicine, *Garcinia hanburyi*, which possesses potent antitumor activity. GA3, a new GA derivative, has been shown to possess better water solubility than GA. The aim of the present study was to examine the antitumor activity of GA3 and the mechanism underlying it.
Methods: The growth inhibition of cancer cell lines induced by GA3 was assessed using the SRB assay. DAPI staining, flow cytometry, a DNA fragment assay, and Western blot analysis were used to study the apoptotic mechanisms of GA3.
Results: GA3 displayed wide cytotoxicity in diversified human cancer cell lines with a mean IC_{50} value of 2.15 μmol/L. GA3 was also effective against multidrug resistant cells, with an average resistance factor (RF) that was much lower than that of the reference drug, doxorubicin. Mechanistic studies revealed that GA3-induced apoptosis in HL-60 cells proceeded *via* both extrinsic and intrinsic pathways, with caspase-8 functioning upstream of caspase-9. In addition, GA3-driven apoptotic events were associated with up-regulation of Bax, down-regulation of Bcl-2 and cleavage of Bid. Moreover, GA3 triggered cytochrome *c* release from the mitochondria, in particular bypassing the involvement of the mitochondrial membrane potential.
Conclusion: Better solubility and a potential anti-MDR activity, combined with a comparable antitumor efficacy, make GA3 a potential drug candidate in cancer therapy that deserves further investigation.

Keywords: gambogic acid; GA3; antitumor; apoptosis; caspase; Bcl-2; cytochrome *c*
Acta Pharmacologica Sinica (2009) 30: 346–354; doi: 10.1038/aps.2009.3

Introduction

Gambogic acid (GA) (Figure 1) is the major active ingredient of gamboges, which is extracted from *Garcinia hanburyi* in Southeast Asia. It has long been used as a folk medicine and coloring agent in China. Pharmacological studies have revealed that GA possesses potent antitumor activity both *in vitro* and *in vivo*[1–3], with the transferrin receptor (TfR) being identified as a favorable target. Binding of GA to the TfR activates the apoptosis cascade using caspase-8 and the mitochondrial pathway. Moreover, Pandey *et al*[4] demonstrated that GA inhibited the NF-kappaB signaling pathway and potentiated apoptosis through its interaction with the transferrin receptor. Recent work in our laboratory further revealed that GA not only displayed potent antiproliferative activity against a panel of human tumors, but also exhibited dramatic anti-MDR activity *in vitro*. Importantly, we proved that GA preferentially functioned as a catalytic inhibitor of human Topo IIα by binding to the ATPase domain[5]. All of these efforts favor GA as a promising anticancer candidate, and it is now under a phase II clinical trial in China.

Although GA has remarkable efficacy against tumors, its poor solubility somewhat limits its appreciable pharmacological profiles in the clinic[6]. As such, a great deal of effort has been made to improve this restriction, in particular for the sake of patients' good compliance. With this in mind, we rationally designed and synthesized a series of new GA derivatives. Encouragingly, *N*-(carboxymethyl)gambogamide (GA3) (Figure 1) stood out as a distinct derivative with better water solubility than the other GA derivatives we synthesized. The solubility has been measured to be more than 3-fold higher than that of GA (aqueous solubility: 0.35

* Correspondence to Prof Jian DING and Wen-hu DUAN.
E-mail jding@mail.shcnc.ac.cn (Jian DING) or whduan@mail.shcnc.ac.cn (Wen-hu DUAN)
Received 2008-11-21 Accepted 2009-01-07

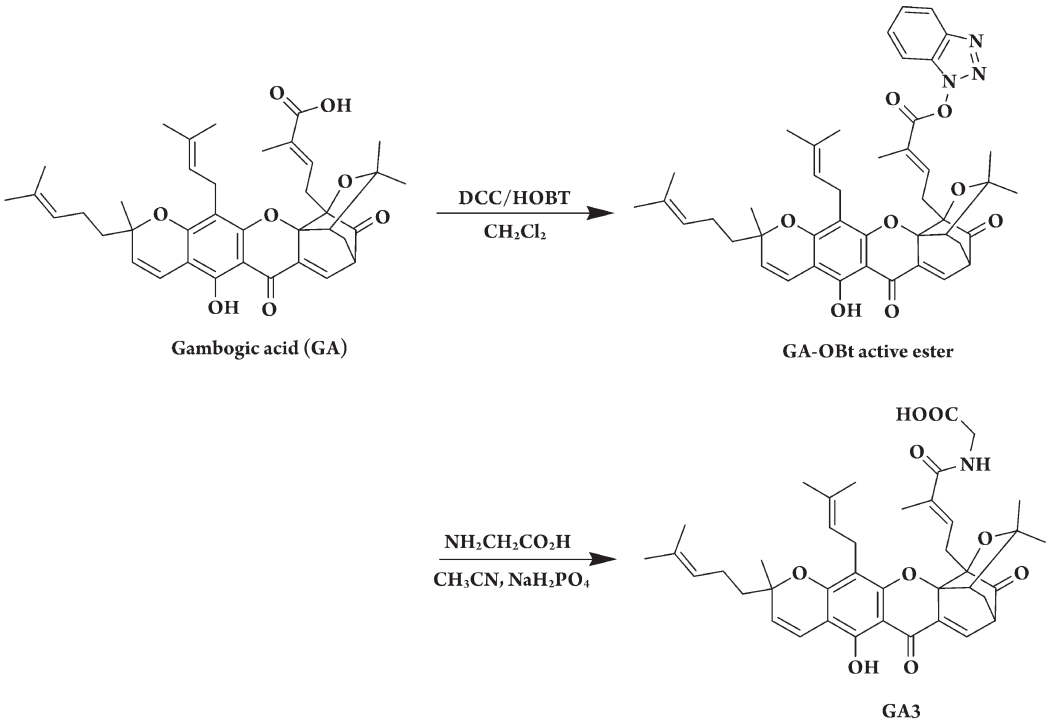

Figure 1. Synthesis of GA3 from GA.

mg/mL for GA3 and 0.11 mg/mL for GA).

In the present study, we demonstrate that GA3 exhibits potent antitumor effects, as well as potential anti-MDR activity, *in vitro*. In addition, GA3 induces caspase-dependent apoptosis in HL-60 cells *via* both extrinsic and intrinsic pathways, with caspase-8 functioning upstream of caspase-9. Thus, comparable anti-tumor efficacy, together with the improved solubility, makes GA3 a potential candidate for future cancer therapy.

Materials and methods

Agents GA3 was structurally modified from the lead compound GA (Figure 1). A mixture of GA, dicyclohexylcarbodiimide, 1-hydroxybenzotriazole (HOBt), and anhydrous dichloromethane was stirred at room temperature for 6 h. The insoluble material was filtered off, and the filtrate was concentrated to dryness. The residue was purified by flash silica gel chromatography with ethyl acetate as an eluent to yield GA-OBt active ester. Glycine and sodium dihydrogen phosphate (NaH_2PO_4) were added to a solution of GA-OBt active ester and acetonitrile, and the resulting mixture was stirred at room temperature for 4 h. The reaction mixture was poured into brine and extracted with ethyl acetate, and the ethyl acetate solution was concentrated to dryness. The residue was purified by flash silica gel chromatography with ethyl acetate and petroleum ether as an eluent to yield GA3 as a yellow gum. The chemical structure of GA3 was confirmed by ^{1}H NMR, EIMS, and elemental analysis. GA3 was dissolved at a concentration of 0.01 M in 100% DMSO as a stock solution.

Caspase inhibitors, Z-VAD-FMK, Z-IETD-FMK and Z-LEHD-FMK were purchased from Calbiochem-Novabiochem Corporation (San Diego, CA, USA). Doxorubicin (DOX) was purchased from Sigma (St Louis, MO, USA).

Cell lines Human gastric adenocarcinoma SGC-7901 and ovarian carcinoma HO-8910 cell lines were obtained from the cell bank of the Chinese Academy of Sciences. Human promyelocytic leukemia HL-60, chronic myelogenous leukemia K562, lymphoblastic leukemia MOLT-4, lung adenocarcinoma NCI-H23, hepatocellular carcinoma HepG2, colorectal adenocarcinoma HT-29 and cervical carcinoma HeLa cell lines were purchased from the American Type Culture Collection. Human gastric adenocarcinoma MKN-28 and MKN-45, colorectal carcinoma HCT-116 and HCT-15, and breast carcinoma MCF-7, MDA-MB-435 and MDA-MB-468 cell lines were obtained from the Japanese Foundation of Cancer Research. DOX-selected multidrug-resistant (MDR) cell sublines K562/A02 and MCF-7/Adriamycin were ordered from the Institute of Hematology,

Chinese Academy of Medical Sciences. All cell lines were maintained in strict accordance with the supplier's instructions and established procedures.

Antibodies The following antibodies were used: anti-caspase 3, anti-poly (ADP) ribose polymerase (PARP), anti-Bid, anti-GAPDH, and anti-actin primary antibodies were obtained from Santa Cruz Biotechnology (Santa Cruz, CA, USA); anti-caspase 8, anti-cleaved caspase 8, anti-caspase 9, anti-Bcl-2, anti-Bax, and anti-cytochrome *c* primary antibodies were obtained from Cell Signaling Technology, Inc (Beverly, MA); and horseradish peroxidase-conjugated secondary antibody was obtained from Pierce Inc (Rockford, IL, USA).

Cell proliferation assay Cell proliferation was evaluated using the SRB assay as previously described[7]. Briefly, cells were seeded into 96-well plates and grown for 24 h. The cells were then treated with increasing concentrations of GA3 and grown for a further 72 h. The medium remained unchanged until the completion of the experiment. The cells were then fixed with 10% precooled trichloroacetic acid (TCA) for 1 h at 4 °C and stained for 15 min at room temperature with 100 μL of 4 mg/mL SRB solution (Sigma) in 1% acetic acid. The SRB was then removed, and the cells were quickly rinsed five times with 1% acetic acid. After cells were air-dried, protein-bound dye was dissolved in 150 μL of 10 mmol/L Tris base for 5 min and measured at 515 nm using a multiwell spectrophotometer (VERSAmax, Molecular Devices). The inhibition rate on cell proliferation was calculated as $(1 - A_{515\ treated}/A_{515\ control}) \times 100\%$. The IC_{50} value was obtained by the Logit method and was determined from the results of at least 3 independent tests. The resistance factor (RF) to each drug was calculated as the ratio of the IC_{50} value of resistant cells to that of parental cells.

DAPI staining assay DAPI staining was performed as described previously[8]. In brief, HL-60 cells (3×10^5 cell/mL) were seeded into 6-well plates and treated with different concentrations of GA3 for the indicated times. The cells were harvested and fixed with 4% paraformaldehyde for 30 min at room temperature. After cells were washed with PBS by centrifugation at 1000×*g* for 5 min, 2 μL DAPI (5 μg/mL) was added to the fixed cells for 5 min, after which they were examined by fluorescence microscopy. Apoptotic cells were identified by condensation and fragmentation of chromatin.

Flow cytometry assay To evaluate the effects of different caspase inhibitors on apoptosis, HL-60 cells (3×10^5 cell/mL) were pre-incubated with or without the inhibitors (50 μmol/L each) for 2 h and then exposed to 2 μmol/L GA3 for 4 h. The cells were harvested and fixed in 70% ethanol and then stored at 4 °C overnight. The cells were then stained in PBS containing 40 μg/mL RNase and 10 μg/mL propidium iodide (PI) at room temperature in the dark for 30 min. Subsequently, the cells were analyzed using a FACS-Calibur cytometer (Becton Dickinson, San Jose, CA, USA). The cells undergoing apoptosis were obtained from the distinct sub-G1 region of the DNA distribution histograms. At least 10 000 events were counted for each sample.

DNA fragments assay DNA fragmentation was extracted using the method given in a previous report[9]. Briefly, after treatment with the control or the desired concentration of GA3 for the specified time interval, HL-60 cells were harvested and lysed with an equal volume of 1.2 % SDS. DNA fragments were isolated in the supernatant by the addition of 7/10 volume of precipitation solution (3 mol/L CsCl, 1 mol/L potassium acetate, 0.67 mol/L acetic acid) and spinning for 15 min at 14 000×*g*; fragments were then absorbed by a miniprep spin column and eluted with 50 μL TE buffer. Purified DNA was electrophoresed using a 1.5% agarose gel and stained with 0.5 μg/mL ethidium bromide to facilitate visualization by fluorescence under UV light.

Measurement of mitochondrial membrane potential (Δψm) Variations in the mitochondrial membrane potential were assessed by flow cytometry using the mitochondrial probes dihexyloxacarbocyanine [$DiOC_6(3)$] and tetrachloro-tetraethylbenzimidazol carbocyanine (JC-1) (Molecular Probes), respectively. HL-60 cells were plated at a density of 3×10^5 cells/well on 6-well plates. After treatment with GA3 (2 μmol/L, 4 h) or the positive control dihydroartemisinin[10] (DHA, 200 nmol/L, 24 h), cells were collected in ice-cold PBS. $DiOC_6(3)$ (40 nmol/L) or JC-1 (1 μmol/L) was loaded into cells suspended in RPMI-1640 medium and incubated at 37 °C for 15 min. Fluorescence was determined using a FACS-Calibur cytometer.

Western blot analysis HL-60 cells (3×10^5 cell/mL) were seeded into 6-well plates and exposed to the indicated concentrations of GA3 for 4 h. After treatment, the cells were collected and then suspended in lysis buffer (100 mmol/L Tris-HCl, pH 6.8, 200 mmol/L DTT, 4% SDS, 0.2% bromophenol blue, 20% glycerol). The cell lysate was cleared by centrifugation at 14 000 r/min for 15 min. Lysate proteins were resolved by sodium dodecylsulfate polyacrylamide gel electrophoresis and transferred onto nitrocellulose membranes. The membranes were incubated for 1 h in 5% milk, followed by 2 h of incubation with primary antibodies. The membranes were washed three times with PBS (with 0.1% Tween-20) and then incubated with the respective peroxidase-conjugated secondary antibody for 1 h. The membranes were washed again three times, developed using enhanced chemiluminescence (ECL, Amersham Biosci-

ences), and then exposed to Kodak X-Omat BT film.

Extraction of cytochrome *c* released into the cytosol After treatment with the control or desired concentration of GA3 for 4 h, the cells were harvested and resuspended in extraction buffer [20 mmol/L HEPES, pH 7.5, 10 mmol/L KCl, 1.5 mmol/L $MgCl_2$, 1 mmol/L EDTA, 1 mmol/L EGTA, 1 mmol/L DTT, 0.1 mmol/L phenylmethylsulfonyl fluoride (PMSF), and 250 mmol/L sucrose] and homogenized. The homogenates were then centrifuged at 750 *g* for 10 min at 4 °C. The supernatants were centrifuged at 10 000 *g* for 15 min at 4 °C, and the remaining supernatant was designated the cytosol fraction. Cytochrome *c* was identified by Western blot analysis with rabbit anti-cytochrome *c* polyclonal antibody from Cell Signaling Technology.

Statistical analysis Data are expressed as the mean±SD from at least three separate experiments, and significance was assessed using a *t* test. Differences were considered significant at $P<0.05$.

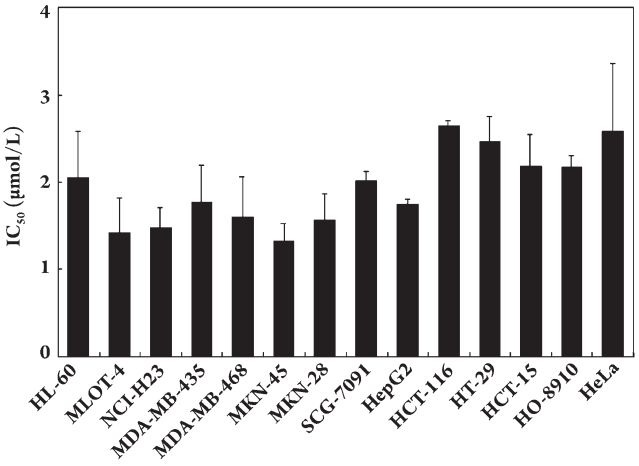

Figure 2. GA3 inhibits proliferation of wide range of human cell lines *in vitro*. Cells in 96-well plates were treated with various concentrations of GA3 for 72 h. Cell viability was determined by sulforhodamine B assay. Three separate experiments were carried out to determine the IC_{50} values. Columns, mean; bars, SD.

Results

GA3 potently inhibits cell proliferation *in vitro* The cytotoxicity of GA3 was evaluated using the SRB assay against a panel of human tumor cell lines including those from leukemia, lung cancer, breast cancer, gastric cancer, hepatocellular cancer, colon cancer, ovarian cancer, and cervical cancer. We found that GA3 produced potent cytotoxicity against a panel of cell lines without distinct selectivity among them, yielding an average IC_{50} of 2.15 μmol/L (Figure 2).

GA3 exhibits anti-MDR activities *in vitro* Because we have reported that GA possesses significant anti-MDR activities, we further tested whether GA3 had the same properties using the two MDR sublines K562/A02 and MCF-7/ADR. Drug-sensitive parental K562 and MCF-7 cell lines and the conventional anticancer drug DOX were used as references. As shown in Table 1, GA3 displayed significant cytotoxicity in the K562/A02 subline examined, with an IC_{50} value of 8.88 μmol/L, similar to that of the parental cell lines (average IC_{50}=6.08 μmol/L). Notably, the resistance factor of GA3 on K562/A02 cells was 1.46, which was much lower than that of the reference drug DOX (RF 55.93). Moreover, the cytotoxicity of GA3 was less potent to the MCF-7/ADR subline (IC_{50} value=25.40 μmol/L) than to the parental cell line (IC_{50} value=5.55 μmol/L). Nevertheless, it was still much more potent than the positive drug DOX, with an average RF of 4.58 for GA3 and 114.25 for DOX.

GA3 induces apoptosis in HL-60 cells Apoptosis has been determined to be responsive to GA-mediated antitumor activities. Accordingly, we investigated the ability of GA3 to induce apoptosis in HL-60 cells using DAPI staining, internucleosomal DNA fragmentation, and flow cytometric analysis.

We first examined the internucleosomal DNA fragmentation at various concentrations of GA3 after different exposure times. In concentration-dependent experiments, we found that treatment with GA3 at concentrations ranging from 0.5 μmol/L to 4 μmol/L for 4 h caused a dose-dependent induc-

Table 1. Cytotoxicity and resistance factors of GA3 and reference drug DOX in MDR and drug-sensitive parental cell lines.

Drug	IC_{50} (mean±SD) (μmol/L)				RF	
	K562	K562/A02	MCF7	MCF7/ADR	K562/A02	MCF7/ADR
GA3	6.08±2.09	8.88±0.35	5.55±0.64	25.40±0.57	1.46	4.58
DOX	0.43±0.17	23.81±2.99	0.39±0.12	44.90±1.27	55.93	114.25

IC_{50} values were determined from 3 separate experiments; each drug concentration was tested in triplicate. The resistance factor (RF) was calculated as the ratio of the IC_{50} value of the MDR cells to that of corresponding sensitive parental cells.

tion of internucleosomal DNA fragmentation. Notably, GA3 at a concentration of 2 μmol/L initiated the DNA ladder fragmentation, and the fragmentation appeared more obviously with increasing concentration, with the maximal effect observed at a concentration of 4 μmol/L (Figure 3A, left). In time-dependent studies, using 4 μmol/L of GA3, we noted that DNA ladder fragmentation was first observed at 2 h and reached the maximum at the 4 h time point (Figure 3A, right).

Next, we focused on the morphological change of apoptosis induced by GA3 using DAPI staining. As shown in Figure 3B, uniform HL-60 cells with normal morphology were observed in control group, whereas HL-60 cells with fragmented chromatin and apoptotic bodies were noted following treatment with 2 μmol/L or 4 μmol/L GA3. These results suggest that GA3 is capable of inducing marked apoptotic morphological changes in HL-60 cells.

To further characterize the apoptosis induced by GA3, we quantified apoptotic cells using flow cytometry analysis. As illustrated in Figure 3C (upper panel), about 20% of the sub G_1/G_0 cells underwent apoptosis following treatment with GA3 at 2 μmol/L for 4 h. More than 60% of HL-60 cells underwent apoptosis when the concentration reaching up to 4 μmol/L. In addition, exposure of HL-60 cells to GA3 (4 μmol/L) for 2 h, 3 h and 4 h triggered time-dependent apoptosis, with treated cells undergoing apoptosis in proportions of 15%, 25% and 60%, respectively (Figure 3C, lower panel).

GA3 activates caspase-3, -8, -9, and induces PARP cleavage We then evaluated whether GA3 induced apoptosis in a caspase-dependent manner. For this experiment, we preferentially examined the impact of GA3 on procaspase-3, an indicator of caspase-3 activity, and the cleavage of PARP, a downstream target of caspase. The results showed that GA3 dose-dependently decreased the expression of procaspase-3 in HL-60 cells. As shown in Figure 4A, procaspase-3 expression declined after exposure to 0.5 μmol/L of GA3 and became undetectable at exposure to 2 μmol/L of GA3. In addition, GA3 resulted in PARP cleavage in a dose-dependent fashion, as evidenced by an increase in 85 kDa of inactive intermediate band of PARP with a concomitant decrease in the 116 kDa of the full length (Figure 4A). Notably, this increased PARP cleavage coincided with increased caspase-3 activation.

To understand the mechanisms involved in the activation of caspase-3, the effects of GA3 on procaspase-8 and procaspase-9 were preferentially examined based on the fact that caspase-3 was activated by caspase-8 and/or caspase-9. As

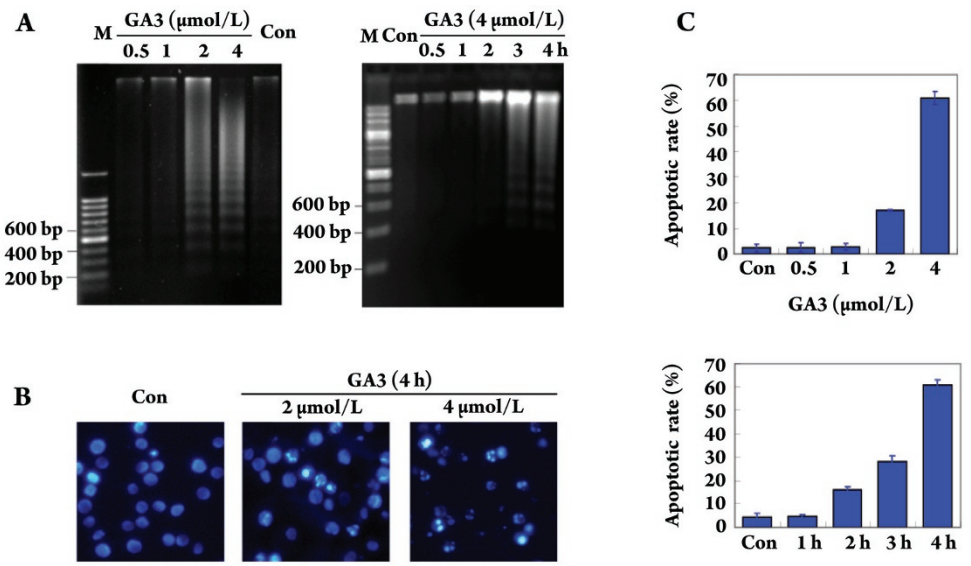

Figure 3. GA3 induces apoptosis in HL-60 cells. (A) Electrophoresis of DNA fragmentation. HL-60 cells were exposed to GA3 at indicated concentrations for 4 h (left) or treated with 4 μmol/L GA3 for indicated times (right), fragmented DNA was extracted and separated in 1% agarose gel electrophoresis. (B) DAPI staining assay. DAPI-stained nuclei of HL-60 cells untreated or treated with 2 μmol/L or 4 μmol/L GA3 were observed using a microcopy (×200). (C) PI staining for flow cytometry. Cells were treated with GA3 for 4 h at indicated concentrations (upper panel) or treated with 4 μmol/L GA3 for indicated times (lower panel). Cells were analyzed using FACS after they were fixed by 70% ethanol and stained with PI. Sub G_0/G_1 DNA content of HL-60 cells were collected as apoptotic cells. The results are typical of those obtained in three independent experiments yielding similar results.

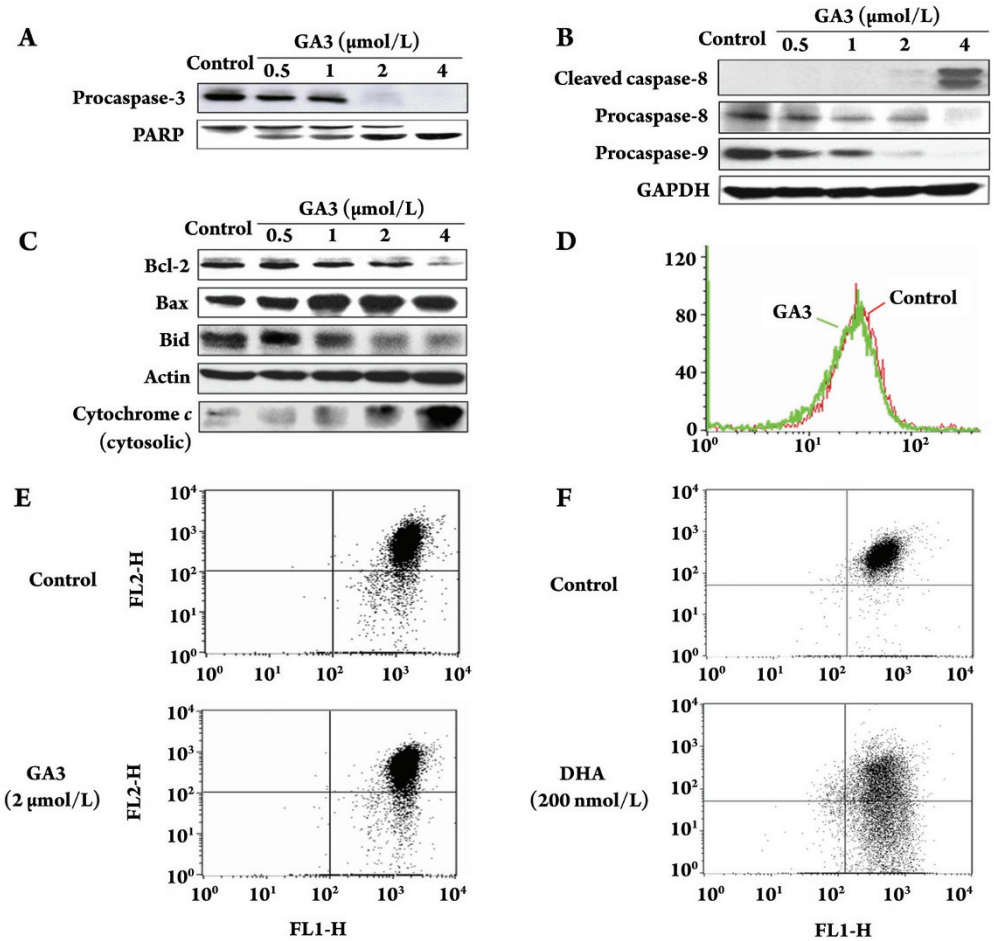

Figure 4. GA3 modulates the expression of apoptosis-related proteins and drives the release of cytochrome *c* without affecting mitochrondrial transmembrane potential. After treatment with control or desired concentration of GA3 for 4 h, HL-60 cells were collected and the activation of caspase-8, -9, -3, cleavage of PARP (A, B), the expression of Bcl-2 family proteins and the release of cytochrome *c* (C) were assayed by Western blotting analysis, respectively. Further, changes in $\Delta\Psi_m$ were assayed. After treatment with 2 μmol/L GA3 for 4 h, HL-60 cells were collected and incubated with $DiOC_6(3)$ (40 nmol/L) (D) or JC-1 (1 μmol/L) (E), respectively, and the $\Delta\Psi_m$ were observed by flow cytometry. Dihydroartemisinin (DHA) (200 nmol/L, 24 h) was used as a positive control (F).

shown in Figure 4B, both initiator caspases were obviously decreased after cells were treated with 0.5 μmol/L of GA3 for 4 h; in particular, these two bands almost completely disappeared when the concentration was increased to 4 μmol/L. These findings favor the involvement of both the extrinsic apoptosis pathway and the intrinsic apoptosis pathway in the GA3-mediated cleavage of caspase-3.

GA3 modulates Bcl-2 family protein expression, drives cytochrome *c* release and the effect is mitochondrial transmembrane potential-independent Bcl-2 family proteins play critical roles in mitochondrial-mediated apoptosis. The Bax:Bcl-2 ratio and Bid cleavage drew our particular interest due to their significance in the mitochondrial-mediated event. Treatment with GA3 caused a marked and dose-dependent decrease in Bcl-2 expression in HL-60 cells but increased the expression of Bax (Figure 4C), which led to an increased ratio of Bax over Bcl-2.

We further investigated the effect of GA3 on Bid, another important Bcl-2 family member that has been demonstrated to relay signals from the cell surface to the mitochondria and result in cytochrome *c* release into the cytosol. Our results indicated that GA3 not only was capable of cleaving Bid (Figure 4C) but also resulted in a significant increase in the release of cytochrome *c* (Figure 4C).

To further elucidate the involvement of the mitochondrial pathway in GA3-induced apoptosis, we next assessed the mitochondrial transmembrane potential ($\Delta\psi_m$) using $DiOC_6(3)$. Unexpectedly, GA3 (2 μmol/L for 4 h) failed to

induce mitochondrial membrane depolarization in any case (Figure 4D), indicating that GA3 was not able to induce the mitochondrial membrane depolarization of HL-60 cells. We then used another commonly accepted mitochondrial probe, JC-1, for further confirmation. Likewise, 4-h treatment with GA3 also caused little change in $\Delta\psi_m$ when compared with the control (Figure 4E). Meanwhile, HL-60 cells treated with DHA, a positive control, exhibited a substantial loss of membrane potential (Figure 4F).

GA3-induced apoptosis proceeds with caspase-8 functioning upstream of caspase-9 The aforementioned findings revealed that the GA3-induced apoptosis-driving event was caspase-dependent in both the death receptor- and the mitochondrial-mediated pathways. This led us to investigate whether these two pathways contributed equally to caspase-driven apoptosis. Using specific inhibitors of caspase-8 and -9 and pan-caspase inhibitor 2 h prior to treatment with GA3 (2 μmol/L, 4 h), we found that Z-VAD-FMK (pan-caspase inhibitor) and Z-IETD-FMK (caspase-8 inhibitor) completely abolished both the GA3-driven DNA fragmentation and the sub-G_0/G_1 increase; the Z-LEHD-FMK (caspase-9 inhibitor), however, failed to block those apoptotic events (Figure 5 A, 5B).

For further confirmation, we performed Western blotting. As we expected, the significant cleavage of PARP and the decreased expression of procaspase-3,-8, and -9 in HL-60 cells induced by GA3 were fully abolished by the concomitant presence of Z-IETD-FMK (Figure 5C). Notably, the GA3-driven decrease in Bid was also abolished by pretreatment with Z-IETD-FMK (Figure 5C).

All of these results clearly indicate that GA3 triggers the caspase-8-mediated extrinsic pathway that functions upstream of caspase-9, which in turn helps to explain the invalidation of the caspase-9 inhibitor in GA3-induced apoptosis in HL-60 cells.

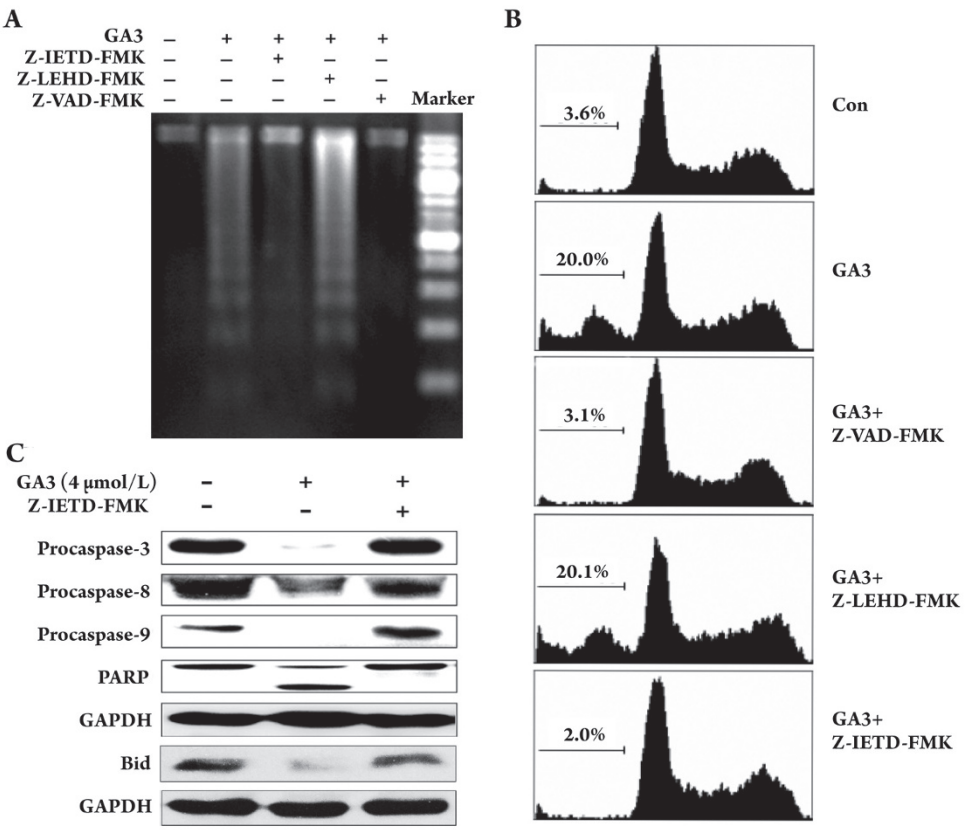

Figure 5. Pan-caspase inhibitor or caspase-8 inhibitor, but not caspase-9 inhibitor, is capable of preventing the GA3-induced apoptosis. After pretreatment with 50 μmol/L pan-caspase inhibitor Z-VAD-FMK, or caspase-8 inhibitor Z-IETD-FMK or caspase-9 inhibitor Z-LEHD-FMK for 2 h, respectively. HL-60 cells were exposed to 2 μmol/L GA3 for 4 h and apoptosis was assayed by DNA fragmentation (A) and flow cytometry after staining with PI (B). (C) GA3-treated HL-60 cells, with or without Z-IETD-FMK pretreatment, were collected and PARP, procaspase-3, -8 and -9 and Bid protein expression were observed by Western blotting.

Discussion

Gambogic acid (GA) is a cytotoxic compound isolated from the gamboge resin of the *Garcinia hanburyi* tree. Investigations indicate that GA may induce apoptosis, repress telomerase activity in cancer cells, inhibit human Topo II catalytic activity, and, thus, exhibit anti-tumor activities both *in vitro* and *in vivo*[1, 2, 5]. GA has now been approved by State Food and Drug Administration of China to be tested in a phase II clinical trial as a new drug to treat cancer. However, the poor solubility of GA somewhat limits its pharmacological profiles. Efforts have been made in our laboratory to design and synthesize new derivatives of GA, with the aim of discovering an innovative antitumor drug candidate with better solubility. GA3 stood out as a distinct derivative possessing better water solubility than GA. In the present study, we proved that GA3 exhibited antitumor activities *in vitro* that are comparable to those of GA[5] *via* apoptosis-involved mechanisms.

Apoptosis is a highly regulated process that involves the activation of a series of molecular events that lead to cell death[11]. Current chemotherapy and radiation therapy are likely to be affected by the apoptotic tendency of cells. As such, apoptosis has favorable therapeutic implications[12, 13]. Current views hold that the caspases played a central role in the execution of apoptosis[14]. However, the apoptotic program is not always just a result of caspase-driven events; in many cell types, activation of the apoptotic program inevitably leads to death, with or without caspase involvement[15]. In this study, pretreatment with Z-VAD-FMK, a pan-caspase inhibitor, significantly inhibited GA3-triggered apoptosis, which favors the notion that GA3 is capable of inducing apoptosis primarily *via* a caspase-dependent mechanism. In general, caspase-driven cascades can be activated through multiple pathways, including a membrane death-receptor pathway utilizing the initiator caspase-8 or through the mitochondrial pathway relying on cytochrome *c* release and thus activation of the initiator caspase-9[14, 16–18]. In the current study, we found that both caspase-8 and -9 could be cleaved and activated upon exposure to GA3, implying that the GA3-induced HL-60 cell apoptosis exhibited both extrinsic and intrinsic pathway dependence. Moreover, the fact that the pan-caspase inhibitor completely abolished DNA fragmentation and the sub-G_0/G_1 increase triggered by GA3, in particular with the notion that the caspase-8 inhibitor blocked but the caspase-9 inhibitor failed to completely abate the DNA fragmentation and sub-G_0/G_1 increase, helps to explain the unequal contribution of these two pathways to GA3-driven events, with caspase-8 functioning upstream of caspase-9.

Addressing the involvement of apoptotic proteins that become activated in response to GA3 will offer a better understanding of how GA3 drives apoptosis. The Bcl-2 family proteins, in particular Bax, Bcl-2 and Bid, draw our preferential attention. Upon apoptosis induction, the Bax in the cytosol is translocated to the mitochondria and executes its pro-apoptotic function[19], whereas Bcl-2 forms heterodimers with Bax to undertake an anti-apoptotic action[20]. In fact, alterations in the levels of Bax and Bcl-2 play paramount roles in determining whether cells will undergo apoptosis. In the present study, we found that GA3-mediated cytosolic cytochrome *c* accumulation paralleled the up-regulation of Bax and the down-regulation of Bcl-2. All of these findings provide strong evidence that the increased Bax/Bcl-2 ratio is responsible for the cytochrome *c* release from mitochondria and thus apoptosis.

Mitochondrial hemostasis is commonly thought to be influenced not only directly by the Bcl-2 family proteins but also indirectly by other mitochondrial proteins, such as the mitochondrial permeability transition pore (PTP). In theory, opening of the PTP quickly leads to $\Delta\psi_m$ decrease, cytochrome *c* release and then apoptotic cell death[21]. Interestingly, our results showed that although GA3 induced significant release of cytochrome *c* from the mitochondria, it exhibited little effect on $\Delta\psi_m$ in HL-60 cells. Although little is known about this seemingly unexpected result, there are emerging data that Bid-induced cytochrome *c* release is mediated independently of PTP[22]. Given that caspase-8 could cleave Bid and activate the mitochondrial pathway[23], that caspase-8 activation was simultaneously accompanied by Bid cleavage in response to GA3 treatment, and, more importantly, that Bid cleavage could be abolished by pretreatment with caspase-8 inhibitor, we are thus encouraged to hypothesize that Bid is critical for GA3-driven cytochrome *c* release, which bypasses the $\Delta\psi_m$/PTP-dependent pathway.

In summary, we validated for the first time the appreciable pharmacological profiles of GA3 identified by its potent antitumor activities, potential anti-MDR capacities, and better solubility than its parent compound GA. The fact that GA3 triggers cytochrome *c* release independent of $\Delta\psi_m$/PTP might provide an alternative view of the GA3-driven apoptotic event in particular. The fact that GA3 (unlike GA) did not cause cell-cycle arrest in tumor cells (data not shown)[24] highlights GA3 as an anti-tumor candidate that is distinct from its parent compound. Additional studies are now underway to further characterize this new compound.

Acknowledgement

This work was financially supported by the National Natural Science Foundation of China (No 30721005). Hua XIE especially appreciated the support from a Shanghai Post-doctoral Grant (No 05R214157).

Author contribution

Hua XIE, Li-ping LIN, Wen-hu DUAN, Jian DING designed research; Hua XIE, Yun-long ZHOU performed research; Lin-jiang TONG contributed new analytical tools and reagents; Hua XIE and Yun-xin QIN analyzed data; Hua XIE, Mei-yu GENG, Wen-hu DUAN, Jian DING wrote the paper.

References

1 Guo QL, You QD, Wu ZQ, Yuan ST, Zhao L. General gambogic acids inhibited growth of human hepatoma smmc-7721 cells *in vitro* and in nude mice. Acta Pharmacol Sin 2004; 25: 769–74.
2 Liu W, Guo QL, You QD, Zhao L, Gu HY, Yuan ST. Anticancer effect and apoptosis induction of gambogic acid in human gastric cancer line bgc-823. World J Gastroenterol 2005; 11: 3655–9.
3 Zhao L, Guo QL, You QD, Wu ZQ, Gu HY. Gambogic acid induces apoptosis and regulates expressions of bax and bcl-2 protein in human gastric carcinoma mgc-803 cells. Biol Pharm Bull 2004; 27: 998–1003.
4 Pandey MK, Sung B, Ahn KS, Kunnumakkara AB, Chaturvedi MM, Aggarwal BB. Gambogic acid, a novel ligand for transferrin receptor, potentiates tnf-induced apoptosis through modulation of the nuclear factor-{kappa}b signaling pathway. Blood 2007; 110: 3517–25.
5 Qin Y, Meng L, Hu C, Duan W, Zuo Z, Lin L, *et al.* Gambogic acid inhibits the catalytic activity of human topoisomerase IIalpha by binding to its atpase domain. Mol Cancer Ther 2007; 6: 2429–40.
6 Han QB, Cheung S, Tai J, Qiao CF, Song JZ, Xu HX. Stability and cytotoxicity of gambogic acid and its derivative, gambogoic acid. Biol Pharm Bull 2005; 28: 2335–7.
7 Skehan P, Storeng R, Scudiero D, Monks A, McMahon J, Vistica D, *et al.* New colorimetric cytotoxicity assay for anticancer-drug screening. J Natl Cancer Inst 1990; 82: 1107–12.
8 Hotz MA, Gong J, Traganos F, Darzynkiewicz Z. Flow cytometric detection of apoptosis: comparison of the assays of *in situ* DNA degradation and chromatin changes. Cytometry 1994; 15: 237–44.
9 Steinfelder HJ, Quentin I, Ritz V. A fast and sensitive technique to study the kinetics and the concentration dependencies of DNA fragmentation during drug-induced apoptosis. J Pharmacol Toxicol Methods 2000; 43: 79–84.
10 Lu JJ, Meng LH, Cai YJ, Chen Q, Tong LJ, Lin LP, *et al.* Dihydroartemisinin induces apoptosis in hl-60 leukemia cells dependent of iron and p38 mitogen-activated protein kinase activation but independent of reactive oxygen species. Cancer Biol Ther 2008; 7: 1017–23.
11 Steller H. Mechanisms and genes of cellular suicide. Science 1995; 267: 1445–9.
12 Fesik SW. Promoting apoptosis as a strategy for cancer drug discovery. Nat Rev Cancer 2005; 5: 876–85.
13 Reed JC. Apoptosis-regulating proteins as targets for drug discovery. Trends Mol Med 2001; 7: 314–9.
14 Riedl SJ, Shi Y. Molecular mechanisms of caspase regulation during apoptosis. Nat Rev Mol Cell Biol 2004; 5: 897–907.
15 Borner C, Monney L. Apoptosis without caspases: an inefficient molecular guillotine? Cell Death Differ 1999; 6: 497–507.
16 Hengartner MO. The biochemistry of apoptosis. Nature 2000; 407: 770–6.
17 Kim KS. Multifunctional role of fas-associated death domain protein in apoptosis. J Biochem Mol Biol 2002; 35: 1–6.
18 Green DR, Reed JC. Mitochondria and apoptosis. Science 1998; 281: 1309–12.
19 Gross A, Jockel J, Wei MC, Korsmeyer SJ. Enforced dimerization of bax results in its translocation, mitochondrial dysfunction and apoptosis. Embo J 1998; 17: 3878–85.
20 Oltvai ZN, Milliman CL, Korsmeyer SJ. Bcl-2 heterodimerizes *in vivo* with a conserved homolog, bax, that accelerates programmed cell death. Cell 1993; 74: 609–19.
21 Gincel D, Zaid H, Shoshan-Barmatz V. Calcium binding and translocation by the voltage-dependent anion channel: a possible regulatory mechanism in mitochondrial function. Biochem J 2001; 358 (Pt 1): 147–55.
22 Kim TH, Zhao Y, Barber MJ, Kuharsky DK, Yin XM. Bid-induced cytochrome *c* release is mediated by a pathway independent of mitochondrial permeability transition pore and bax. J Biol Chem 2000; 275: 39474–81.
23 Yin XM, Wang K, Gross A, Zhao Y, Zinkel S, Klocke B, *et al.* Bid-deficient mice are resistant to fas-induced hepatocellular apoptosis. Nature 1999; 400: 886–91.
24 Yu J, Guo QL, You QD, Zhao L, Gu HY, Yang Y, *et al.* Gambogic acid-induced G_2/m phase cell-cycle arrest via disturbing cdk7-mediated phosphorylation of cdc2/p34 in human gastric carcinoma bgc-823 cells. Carcinogenesis 2007; 28: 632–8.